International Journal for Research in Engineering Application & Management (IJREAM)
ISSN : 2454-9150 Special Issue - AMET-2019

Material Improvement of Actuators: A Review

Nitish S. Vazalwar, Department of Mechanical Engineering, MIT-COE, Pune, India
Sumedh M. Vaidya, Department of Mechanical Engineering, MIT-COE, Pune, India
Jay U. Panchpor, Department of Mechanical Engineering, MIT-COE, Pune, India
Kaivalya S. Patkar, Department of Mechanical Engineering, MIT-COE, Pune, India
Sachin R. Gore, Assistant Professor, Department of Mechanical Engineering, MIT-COE, Pune, India

Abstract: The paper gives an overview of the actuators- components actually responsible for movement in the machines we see around us. The seminar touches the history, advantages and limitations briefly. Used extensively in almost every field of engineering, medical, the study and subsequent improvement of the actuator is of paramount importance. The paper focuses specifically on two aspects of the multifaceted domain of improvement and optimizing of actuators- first, improvement in the material used for actuators and then scope of improvement in design. Furthermore, a case study in form of electric motor of vehicle wheel is discussed.

Keywords — Actuator, Coreless, Design, Graphene, Improvement, Material, Nanotubes

I. INTRODUCTION

The actuation systems gained significantly around World War II. Mainly hydraulic and pneumatic actuations were in use which were improved in terms of their performance by Xhiter Anckeleman in 1938. It was aimed for highest braking force while reducing wear and tear in the automobile. The types are-

Hydraulic

A hydraulic actuator consists of an apparatus that uses fluid power to facilitate translational or rotational operations. The mechanical motion gives an output in terms of linear, rotatory or oscillatory motion. As liquids are nearly impossible to compress, a hydraulic actuator can exert a large force. The drawback of this approach is its limited acceleration.

Pneumatic

A pneumatic actuator converts energy using compressed air at high pressure into linear or rotary motion. Pneumatic system is a rapid action system that is used for engine controls. Pneumatic actuators produce large forces from small pressure changes.

Thermal or Magnetic

Thermal actuators tend to be compact, lightweight, economical and with high power density. These actuators use shape memory materials (SMMs), such as shape memory alloys (SMAs) or magnetic shape-memory alloys (MSMAs). Some popular manufacturers of these devices are Finnish Modti Inc., American Dynalloy and Rotork.

Mechanical

A mechanical actuator converts one kind of motion, such as rotary motion, into another kind, such as linear motion. An example is rack and pinion. The operation of mechanical actuators is based on combinations of structural components.

II. MATERIAL IMPROVEMENT

Traditionally actuators are made of typical metal or plastics. Changing the base material for improving actuator performance gives tremendous results. Although not a new concept, graphene sheets are used to fabricate actuators. This avenue of research continues to give superb results and new research is always developed.

Graphene Sheets

Paper like materials made of stacked graphene oxide platelets produced by filtration of a liquid graphene oxide suspension shows better mechanical properties, with a modulus of about 40 GPa and a fracture strength of 130 GPa. Chemical changes of graphene oxide paper with divalent ions enhance its mechanical properties. Graphene Oxide (GO) is generated by oxidizing graphite and contains oxygen groups such as hydroxyl and epoxy groups on the base plane and –COOH groups on the edges. This makes GO hydrophilic. The oxygen functional groups in GO which contain layered structure, allow dynamic intercalation of water molecules. Interlayer distance varies reversibly between 6-12 A^{o} depending upon relative humidity.

The use of two different building blocks is a useful approach in fabricating mechanical actuators. The Texas

Materials Institute, created "paper" bilayer samples composed of a layer of crisscrossed GO sheets. Studies were carried out for potential use in NEMS, sensors, composites and actuators.

Both GO and CNT's are composed of same base material of sp^2 hybridized carbon atoms so structural compatibility is possible between them. Stable interference can be obtained. [1]

Observations Made at University of Texas

- Surface of GO was dark brown and electrically insulating. (as opposed to CNTs which are black and shiny)
- Surfaces of GO and CNT do not contaminate each other
- Bilayer is flexible
- GO bilayer shrink and increase with change in relative humidity [2]

Inference

- Possibility of application in wrapping and storage
- An actuator for relative humidity [2]

III. Experiment of Sensitiveness to Relative Humidity (R.H.)

Experimental Section

Method: Hummers method was used to synthesize GO (SP-1, Bay Carbon, and MI). Colloidal suspensions (30 mg of GO per 10 mL of water) of individual graphene oxide platelets in purified water (17.4 MV resistance) were prepared with the aid of ultrasound in 20-mL batches. Aqueous colloidal suspensions of MWCNTs were prepared by probe sonication of the mixture with COOH-functionalized CNTs (10 mg of MWCNT in 150 mL of water, NANOLAB, >95%, diameter: 15_5 nm, length: 5–20 mm) and hexadecyl trimethyl ammonium bromide (100 mg for10 mg of MWCNTs, >99% from Fluka) for 24 h. Both homogenous graphene oxide and MWCNT paper samples were made by filtration of the resulting colloidal suspension through an Anodic membrane filter (47 mm in diameter, 0.02-mm pore size, Whatman, Middlesex, UK). The bilayer paper was produced by sequential filtration of MWCNTs and then graphene oxides, aqueous colloidal suspensions suspension through an Anodic membrane filter (47 mm in diameter, 0.02-mm pore size, Whatman, Middlesex, UK). The resulting bilayer papers were rinsed by addition of purified water and filtered 3 times. After the filtration, the papers were suction-dried for half a day, followed by a thorough wash, soaked in purified water for half a day each time (3 times) before being peeled from the filter.

Instruments: The secondary electron images of the bilayer paper sample were taken with a FEI Quanta-600 FEG Environmental SEM using a voltage of 10 to 15 keV. Temperature measurements were made with ThermoTrace 15006 from DeltaTRAK. Relative humidity was measured with Caliber III by WESTERN. The TGA of the paper samples was measured by PERKIN-ELMER TGA with 1 o min_1 heating rate in the air flow.

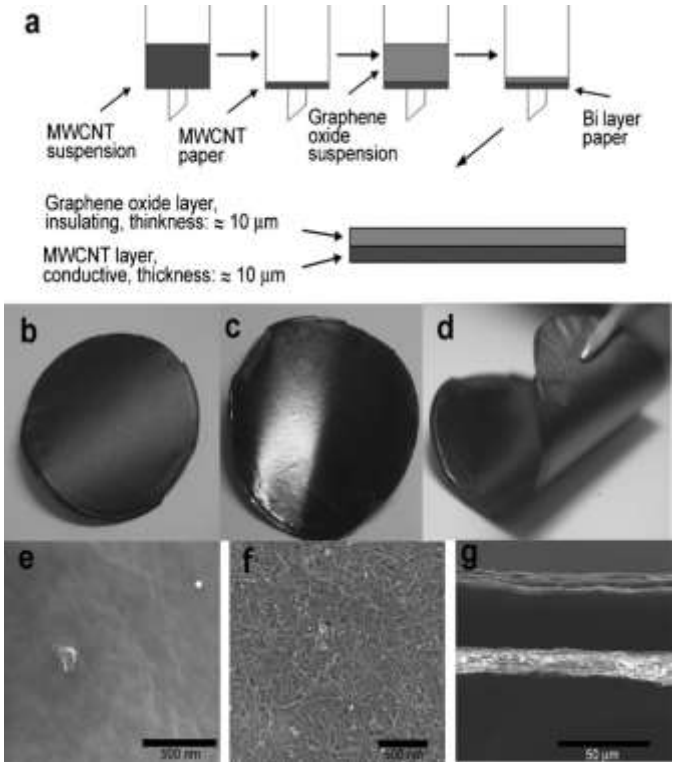

Fig. 1

a) Schematic drawing of how the bilayer paper is made. B–d) Photos of both surfaces

Of the bilayer paper. b) Graphene oxide layer and c) MWCNT layer. d) Curled bilayer paper,

Outside: graphene oxide layer, inside: MWCNT layer. E–g) SEM images of the surface.

e) Graphene oxide layer and f) MWCNT layer. g) SEM image of the cross-section of the bilayer

Paper; upper layer: MWCNT and lower layer: graphene oxide [4]

CARBON NANOTUBE NANO MOTOR

Nanotube Nano motor is a device generating linear or rotational motion using carbon nanotube(s) as the primary component. Nature has some of the most efficient and powerful Nano motors. Some of these have been re-engineered to serve desired purposes. However, these are designed to work in specific environmental. Laboratory-made Nanotube Nano motors on the other hand are more robust and can operate in diverse environments including varied frequency, temperature, mediums and chemical environments. The vast differences in dominant forces and criteria between macroscale and micro/Nanoscale offer new options to construct made to order Nano motors. [4]

Electrostatic forces

Coulomb's law states that the electrostatic force between two objects is inversely proportional to the square of their distance. Hence, as the distance is reduced to less than a few micrometers, a large force can be generated from very small charges on two bodies. However, electrostatic charge scales four times, hence the electrostatic force also scales four times. [4]

Friction

Frictional force scale in a quadratic manner with size $F \sim L^2$. Friction is an ever-present problem regardless of the scale of a device. It becomes more dominant when a device is scaled down. NEMS devices typically have a very large surface area-to-volume ratio. Surfaces in the nanoscale resemble a mountain range, where each peak corresponds to an atom or a molecule. Friction at the nanoscale is proportional to the number of atoms that interact between two surfaces. Hence, friction between perfectly smooth surfaces in the macroscale is actually similar to large rough objects rubbing against each other.

In the case of nanotube nano motors however, the inter shell friction in the multi-walled nanotubes (MWNT) is negligible. Studies show that, with the exception of small peaks, the frictional force remains almost negligible for all sliding velocities until a key sliding velocity is achieved. Simulations relating the sliding velocity, induced rotation, inter-shell frictional force to the applied force explain the low inter-wall friction. Unlike the macroscale expectations the speed at which an inner tube travels within an outer tube does not follow a linear relationship with the applied force. Instead, the speed remains constant even if applied force increases, sometimes in step fashion. No rotation is noticed in non-chiral inner tubes. In the case of chiral tubes, a rotation is noticed and the angular velocity also jumps to match with the jumps in the linear velocity. These plateaus and jumps can be explained as a natural outcome of frictional peaks for growing velocity, the rising side of the peak leading to a plateau, the dropping side leading to a jump. These peaks occur due to excitation of vibrational modes in the walls of the tubes due to the sliding of the inner tube. With the exception of small peaks that correspond to the speed plateaus the frictional force remains at a small numerical value for all sliding velocities until a special sliding velocity. These velocity plateaus correspond to the peaks in the frictional force. [3]

First NEMS Nano Motor

The first nano motor is just a scaled down version of a comparable microelectromechanical systems (MEMS) motor. The nano actuator consists of a gold plate rotor, rotating about the axis of MWNT. The ends of the MWNT rest on a Silicon dioxide layer which form the two electrodes. Three fixed stator electrodes surround the rotor assembly. Four independent voltage signals are applied to control the position, velocity and direction of rotation. Empirical angular velocities recorded provide a lower bound of 17 Hz during complete rotations. It is however, capable of working at considerably high frequencies than just 17 Hz. [1]

Fabrication

The MWNTs are synthesized by the arc-discharge technique with 1, 2-dichlorobenzene as suspension medium and deposited on extremely low doped silicon substrates with a 10^{-6}m of SiO_2. The MWNT can be aligned to match the markings made earlier on the substrate by using an atomic force microscope (AFM) or a scanning electron microscope (SEM) instruments. The rotor, electrodes and the stators are patterned using electron beam lithography using an appropriately masked photo-resist. Gold with a chromium layer to provide required adhesion, is thermally evaporated, acetone being used in the process, and then annealed at 400 °C to ensure better electrical and mechanical contact with the MWNT. The rotor measures 250–500 nm on a side. An HF etch is then used to remove sufficient thickness, approximately 500 nm of SiO_2, of the substrate to make room for the rotor when it rotates. The Si substrate acts as the gate stator. The MWNT at this point displays a very high torsional spring constant (10^{-15} to 10^{-13} N m with resonant frequencies in the tens of megahertz), hence, not allowing large angular displacements. To overcome this, one or more outer MWNT shells are removed in the region between the anchors and the rotor plate. The smaller nanotube(s) are fabricated using the Electrical driven vaporization. Passing current between the two electrodes usually results in failure of the outermost shell only on one side of the nanotube. Current is therefore passed between one electrode and the center of the MWNT which results in the failure of the outermost shell between this electrode and the center. The process is repeated on the opposite side to result in the formation of the short concentric nanotube. It thus behaves like a low friction bearing along the longer tube. [1]

Arrays of Nano Actuators

Due to the extremely low magnitude of output generated by a single nano actuator it is necessary to use arrays of such actuators to accomplish a higher task. Conventional methods like chemical vapor deposition (CVD) allow the exact placement of nanotubes by growing them directly on the substrate. However, such methods are unable to produce very high qualities of MWNT. Also, CVD is a high temperature process that would adversely affect the compatibility with other materials in the system. A Si substrate is coated with electron beam resist and soaked in acetone to leave only a thin layer. The substrate is selectively exposed to a low energy electron beam of a SEM for the activation of the adhesive properties of the polymer.

The alignment method uses the surface velocity obtained by a fluid as it flows off a spinning substrate. MWNTs are suspended in ortho dichlorobenzene (ODCB) by ultra-sonication in an aqua sonic bath that separates most MWNT bundles into individual MWNTs. Drops of this suspension are then pipetted one by one onto the center of a silicon substrate mounted on a spin coater rotating at 3000 rpm. Each subsequent drop of the suspension is pipetted only after the previous drop has completely dried to ensure larger density and better alignment of the MWNTs. Standard electron beam lithography is used to pattern the remaining components of the nano actuators. [4]

Arc-Discharge Evaporation Technique

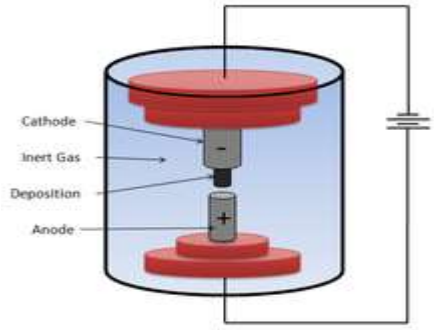

Fig. 2 Cartoon showing the basic experimental setup for the arc-discharge technique of large-scale carbon nanotube synthesis

This technique is a variation of the standard arc-discharge technique used for the synthesis of fullerenes in an inert gas atmosphere. As Figure 1.3 shows, the experiment is carried out in a reaction vessel containing an inert gas such as helium, argon, etc. at a constant pressure. A potential of around 18 V is applied across two graphite electrodes separated by a short distance. The high amount of current passed through the electrodes ensures nanotube formation. As a result, carbon atoms are ejected from the anode and are deposited onto the cathode hence shrinking the mass of the anode and increasing that of the cathode. The black carbonaceous deposit is seen growing on the inside of the cathode while a hard-grey metallic shell forms on the outside. The total yield of nanotubes as a proportion of starting graphitic material peaks at a pressure of 500 torr. The nanotubes formed range from 2 to 20 nm in diameter and has varied length. There are several advantages of choosing this method over the other techniques such as laser ablation and chemical vapor deposition such as

- fewer structural defects
- better electrical, mechanical and thermal properties,
- high production rates [4]

Electrical-Breakdown Technique

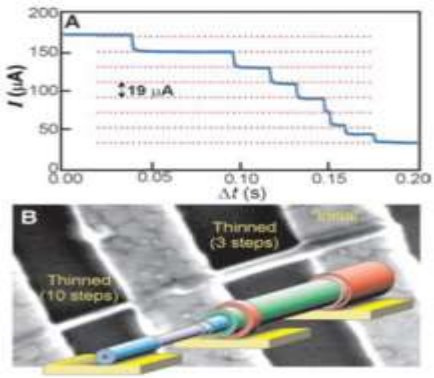

Fig. 3 (A) Graph showing remarkably discrete, constant drops in conductance for the removal of each subsequent carbon shell under constant voltage (B) Images of partially broken MWNTs show clear thinning, with a decrease in radius equal to the inter shell spacing (0.34 nm) times the number of completed breakdown steps. The two segments of this sample were independently thinned by 3 and 10 shells, as depicted by the color overlays [3]

Large-scale synthesis of carbon nanotubes typically results in a randomly varied proportion of different types of carbon nanotubes. Some may be semiconducting while others may be metallic in their electrical properties. Electrical-breakdown technique provides a means for the selection as well as separation of required type of nanotubes. Carbon nanotubes are known to withstand very large current densities up to 10^9 A/cm^2 due to the strong sigma bonds between carbon atoms. However, at sufficiently high currents the nanotubes fail due to rapid oxidation of the outermost shell. This results in a partial conductance drop. Applying an increased bias displays multiple independent and stepwise drops in conductance (figure 1.4) resulting from the sequential failure of carbon shells. Current in a MWNT typically travels in the outermost shell due the direct contact between this shell and the electrodes. This controlled destruction of shells without affecting disturbing inner layers of MWNTs permits the effective separation of the nanotubes. [3]

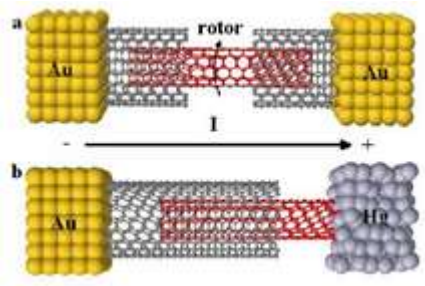

Fig. 4 Nano motor and Nano Drill

Electron windmill

Structure

As figure shows, the nano motor consists of a double-walled CNT formed from an achiral outer tube fixed to external

gold electrodes and a narrower chiral inner tube. The central portion of the outer tube is removed using the electrical-breakdown technique to expose the free-to-rotate, inner tube. The nano drill also has an achiral outer nanotube attached to Au electrode but the inner tube is connected to Hg bath. [1]

Principle

Conventional nanotube nano motor uses of static forces like elastic, electrostatic, friction and van der Waals forces. The electron windmill model makes use of a new "electron-turbine" drive mechanism that eliminates the need for metallic plates and gates that the above nano actuators require. When a DC voltage is applied between the electrodes, a "wind" of electrons is produced from left to right. The incident electron flux in the outer tube initially possesses zero angular momentum, but acquires a finite angular momentum after interacting with the inner tube. By Newton's third law, this a torque on the inner nanotube causing it to rotate hence giving this model the name – "electron windmill". For moderate voltages, the tangential force produced by the electron wind is much greatly exceed the associated frictional forces. [1]

Applications

Some of the main applications of the electron windmill include:

1. A voltage pulse could cause the inner element to rotate at a calculated angle hence making the device behave as a switch or a nanoscale memory element.
2. Modification of the electron windmill to construct a nano fluidic pump by replacing the electrical contacts with reservoirs of atoms or molecules under the influence of an applied pressure difference. [1]

IV. CONCLUSION

Thus, object of this paper is to present to sides of the same coin, which is optimizing and improving the performance of actuators.

Furthermore, actuators are an integral part of the sensing and actuation module of a mechatronic system. Improving in the performance of actuators calls for improvement in the sensors. Conversely, if there is a key development in the area of sensors, it is bound to have a positive effect on the actuator component.

All the major fields of engineering as well as medical are going to be affected by the development in this field.

REFERENCES

[1] Bailey, S. W. D.; I. Amanatidis; C. J. Lambert (2008) Carbon Nanotube Electron Windmills: A Novel Design for Nano motors; Physical Review Letters.

[2] Zettl group http://www.physics.berkeley.edu/research/zettl/project

[3] Carbon Nanotube Actuators R. H. Baughman, C. X. Cui, A. A. Zakhidov, Z. Iqbal, J., N. Barisci, G. M. Spinks, Gordon Wallace, A. Mazzoldi, D. de Rossi, A. G. Rinzler, O. Jaschinski, S. Roth, and M. Kertesz

[4] Design Considerations for Coreless Linear

[5] Actuators Maarten F. J. Kremers, Johannes J. H. Paulides, Jeroen L. G. Janssen, and Elena A. Lomonova Eindhoven, University of Technology, Eindhoven 5612AZ, The Netherlands

[6] J. de Boeij, E. Lomonova, A. Vandenput, "Modeling ironless permanent-magnet planar actuator structures", IEEE Trans. Magn., vol. 42, no. 8, pp. 2009-2016, 2006.

[7] M. Platen, G. Henneberger, "Examination of leakage and end effects in a linear synchronous motor for vertical transportation by means of finite element computation", IEEE Trans. Magn., vol. 37, no. 5, pp. 3640-3643, 2001.

[8] J. L. G. Janssen, J. J. H. Paulides, E. A. Lomonova, "Three-dimensional analytical field calculation of pyramidal-frustum shaped permanent magnets", IEEE Trans. Magn., vol. 45, no. 10, pp. 4628-4631, 2009.

[9] J. Maridor, M. Markovic, Y. Perriard, D. Ladas, "Optimization design of a linear actuator using a genetic algorithm", Proc. IEEE Int. Electric Machines and Drives Conf. IEMDC '09, pp. 1776-1781, 2009.

[10] J. Faiz, M. Ebrahimi-Salary, G. Shahghplian, "Cogging force alleviation in linear permanent magnet generators", AFRICON, pp. 1-6, 2009-Sep.

[11] J. W. Jansen, J. L. G. Janssen, J. M. M. Rovers, J. J. H. Paulides, E. Lomonova, "(Semi-) analytical models for the design of high-precision permanent magnet actuators", Int. Compumag Soc. Newsletter, vol. 16, no. 2, pp. 4-17, 2009.

[12] E. P. Furlani, Permanent Magnet and Electromechanical Devices: Materials Analysis and Applications, U.K., London:Academic, 2001.

[13] K. Halbach, "Design of permanent multipole magnets with oriented rare earth cobalt material", Nucl. Instrum. Methods, vol. 169, no. 1, pp. 1-10, 1980.

[14] É. Durand, Magnétostatique, Paris:Masson, 1968